Article:
Yahya, SG, Mao, X and Jaworski, AJ (2017) Experimental investigation of thermal performance of random stack materials for use in standing wave thermoacoustic refrigerators. International Journal of Refrigeration, 75. pp. 52-63. ISSN 0140-7007

https://doi.org/10.1016/j.ijrefrig.2017.01.013

Accepted Manuscript

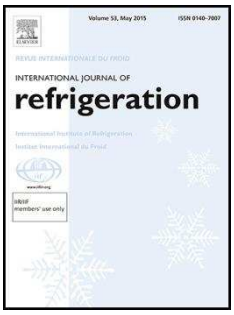

Title: Experimental investigation of thermal performance of random stack materials for use in standing wave thermoacoustic refrigerators

Author: Samir Gh. Yahya, Xiaoan Mao, Artur J. Jaworski

PII: S0140-7007(17)30025-7
DOI: http://dx.doi.org/doi: 10.1016/j.ijrefrig.2017.01.013
Reference: JIJR 3525

To appear in: International Journal of Refrigeration

Received date: 10-1-2017
Accepted date: 15-1-2017

Please cite this article as: Samir Gh. Yahya, Xiaoan Mao, Artur J. Jaworski, Experimental investigation of thermal performance of random stack materials for use in standing wave thermoacoustic refrigerators, International Journal of Refrigeration (2017), http://dx.doi.org/doi: 10.1016/j.ijrefrig.2017.01.013.

Experimental investigation of thermal performance of random stack materials for use in standing wave thermoacoustic refrigerators

Samir Gh. Yahya, Xiaoan Mao and Artur J. Jaworski*

Faculty of Engineering, University of Leeds, Leeds LS2 9JT, United Kingdom

*Corresponding author: a.j.jaworski@leeds.ac.uk ; Tel: +44(0)113-343-4871

Highlights

- Random materials considered for stacks in thermoacoustic refrigerators
- Steel wool, copper scourers and RVC foam compared to plate stacks
- Thermodynamic performance of random materials tested
- COP, COPR and temperature difference vs. cooling load quantified
- Maximum COPR vs. ratio of hydraulic radius to thermal penetration depth established

Abstract

In a standing wave thermoacoustic refrigerator, heat transport from the "cold" to the "ambient" end of a stack is achieved by means of an oscillatory motion of a compressible fluid undergoing cyclic compression and expansion. However, the stacks can be both costly and impractical to fabricate due to material and assembly costs, which limits the cost benefits of thermoacoustic systems. Some of these problems could be solved by the application of stacks that have irregular geometries, for instance stacks made of "random" materials from metal machining (swarf), which are often considered as waste. In this paper, the thermal performance of stacks made of a few selected materials is determined by carrying out experiments in a standing wave thermoacoustic refrigerator. The reported results will be beneficial for developing low-cost thermoacoustic refrigerators or heat pumps for both domestic and commercial applications.

Keywords: Thermoacoustic refrigerators; Standing wave; Thermoacoustic stacks; Random materials; Thermal performance

Nomenclature

A	Cross sectional area
A_{spk}	Cross sectional area of diaphragm of a loudspeaker
A_{wet}	Total wetted area of a stack
c_p	Thermal capacity of fluid
F	Frequency
K	Thermal conductivity
m_{solid}	Mass of solid material
p	Acoustic pressure amplitude
Q	Cooling load
r_h	Hydraulic radius
T_c	Temperature of the cold reservoir
T_h	Temperature of the hot reservoir
U	Volumetric velocity amplitude
V_{gas}	Volume of gas in a stack
V_{solid}	Volume of solid material in a stack
V_{tot}	Total volume of a stack, = V_{gas} + V_{solid}
W_{ac}	Acoustic power
δ_v	Viscous penetration depth
δ_κ	Thermal penetration depth
μ	Dynamic viscosity of fluid
ξ	Displacement amplitude
Π	Perimeter
ρ	Density of fluid
ρ_{solid}	Density of solid material
σ	Absolute uncertainty
Φ_{pU}	Phase difference between acoustic pressure and volumetric velocity
$\Phi_{p\xi}$	Phase difference between acoustic pressure and displacement
ω	Angular frequency
COP	Coefficient of Performance
COPC	Carnot Coefficient of Performance

COPR	Relative Coefficient of Performance
PPI	Pores per inch

1. Introduction

Thermoacoustic refrigerators and engines are a group of systems that make use of "thermoacoustic effect" to achieve energy conversion between thermal and acoustic power. They rely on the interaction between the compressible fluid undergoing an acoustic oscillation and solid structures, such as stacks (the name "stack" being typically associated with standing wave systems) and regenerators (typically in travelling wave systems) that are placed in the resonator. In the last two decades, thermoacoustic devices have attracted a lot of attention because their only moving mechanical component are acoustic drivers, (the oscillating working gas under the acoustic excitation executing the thermodynamic process). The absence of mechanical moving parts and the associated dynamic seals and lubrication gives a great advantage to thermoacoustic devices over many other conventional energy conversion devices, especially in terms of high reliability and minimal maintenance. The working gas in thermoacoustic devices is usually one of the noble gases or their mixture, and sometimes air, making this technology also environmentally friendly.

However, achieving a high efficiency system remains one of the many challenges facing this relatively new technology before it can be applied more widely in industry. A systematic design and optimization algorithm was proposed for thermoacoustic refrigerators, based on the short stack boundary layer approximation (Wetzel and Herman, 1997). Simulations based on the same approximation indicate that refrigeration, including air conditioning and cryogenic cooling, is the best application of thermoacoustic cycles in terms of high efficiency (Paek et al., 2007). Several pieces of work were also devoted to a better understanding of how each of the essential components of the system performs, for example the stack (Tijani et al, 2002) or the regenerator (Backhaus and Swift, 2001). The impact of the

operating frequency and temperature difference between the stack ends on the refrigeration power was studied using network and thermodynamic models, as well as experimental approaches (Jebali et al., 2004). Another important strand of research involves looking at the physics of the thermoacoustic effect, for example the experimental demonstration of the thermoacoustic effect (Biwa et al., 2004) and the nonlinear acoustic streaming that often takes place in such systems (Bailliet et al., 2001).

In parallel to the studies into the improvement of system efficiency by a careful design of all components, efforts are also made to develop systems that are low-cost but of an equivalent or marginally lower efficiency (Saechan et al., 2011). One component of particular concern is the stack/regenerator, because the fabrication of stacks, such as those made out of thin parallel sheets, is usually costly and impractical, while using pre-fabricated stacks, for example ceramic catalytic converter substrates used in the automobile industry, has high materials costs, which limits the cost advantages of thermoacoustic devices as well as pre-defined hydraulic radii, unsuitable for high pressure devices. Some of these problems could be avoided if irregular stack geometries made out of random (very often waste) materials could be used. There is a wide range of such candidate materials, including steel wool and waste material from metal machining (swarf, scourers) and others. However the main difficulty is the lack of experimental data characterising the performance of such stacks at the design stage. The performance of some of these material used as regenerators in the travelling wave thermoacoustic devices has been recently studied by Abduljalil et al. (2011).

In many thermoacoustic engines, generators and refrigerators, noble gases and their binary mixtures are often used to meet the requirement for low Prandtl number, a high thermal conductivity, a high speed of sound and a large specific heat ratio. However, in view of the high costs of noble gases, air is considered a more economic and easily available alternative to be used as the working medium

(Jaworski and Mao, 2013). Hence, air is used as the working gas in the work presented here. In this paper, a study of the performance of a standing wave thermoacoustic refrigerator with a stack made out of several types of random materials is reported. The results from this work are thought to be of particular benefit for the development of low-cost thermoacoustic coolers, heat pumps or prime movers for both domestic and commercial applications.

2. Experimental apparatus and instrumentation

The experimental apparatus consists of a straight square cross-sectional resonator, with one end attached to an acoustic driver (loudspeaker) via a transition section, and another end attached to a compliance "box" via a second transition section, as indicated by the photograph and schematic diagram of the experimental apparatus in Fig. 1. The resonator is a 1.82 m long duct of 76.2 mm × 76.2 mm in cross section. The acoustic driver is a subwoofer type loudspeaker (Precision Device Model 1850), which can nominally produce up to 800 watts of acoustic power. It is connected with the resonator through a square plate with a circular cut-out to match the loudspeaker aperture and a square cross-section transition, to match the resonator on one end and the plate on the other.

The transition section on the far end from the loudspeaker is made of two parts. The first part has a 50 mm long straight section of the same cross section as that of the duct. The second part forms a smooth transition of the cross-sectional area from 76.2 mm × 76.2 mm to 260 mm × 260 mm. The compliance "box" is made of mild steel and has dimensions 300 mm × 300 mm × 280 mm. It is used to simulate a velocity antinode or a pressure node, which will be confirmed by measurements. The resonator is filled with air at atmospheric pressure and room temperature.

The apparatus is operated at its fundamental resonance frequency of 72 Hz and a half-wavelength standing wave is established in the resonator. In this configuration, a low acoustic impedance is created on the driver end, which is favourable to the loudspeaker used in this study. The configuration also helps to suppress the harmonic content so that the acoustic wave remains sinusoidal. It's worth noting that the loudspeaker-type acoustic driver used is not optimal in terms of converting electrical power to acoustic power at the created acoustic condition. Nevertheless, its capability is sufficient for undertaking the measurements required by this study.

The stack sample under test is placed in the resonator with its midpoint 1393 mm away from the loudspeaker. Each of the stacks has the same dimension of 76 mm × 76 mm × 150 mm. An ambient heat exchanger (AHX) is placed next to the hot end of the stack to remove heat from the thermoacoustic system. It comprises of an array of brass fins joined together by soft soldering, as shown in Fig. 1C. The fin thickness is 1 mm, with 3 mm gaps between fins, which makes 59 % of the total cross sectional area open to the oscillating air inside the resonator. Cooling water passes through the flow passages in the ambient heat exchanger to maintain the temperature at the hot end of the stack at 22 ºC. A cold heat exchanger (CHX) is placed next to the cold side of the stack. It is an electrical heater (cf. Fig. 1C) made of resistive wire wound around ceramic pillars, acting as a cooling load. The heating power applied to the heater, which becomes the cooling load on the thermoacoustic stack, is controlled by a direct-current power supply and can be easily varied during the measurements. The value of the cooling load can be obtained directly from the readings on the power supply. Both heat exchangers are 20 mm long in the acoustic propagation direction.

Temperatures on both ends of the stack are measured with K-type thermocouples. The acoustic pressure in front of the moving diaphragm of the loudspeaker is measured with a dynamic pressure transducer

(PCB Model 106B50), and the displacement of the diaphragm is measured with a high speed laser displacement sensor (Keyence LK-G3001P). The pressure and displacement signals acquired simultaneously are converted to signals in the frequency domain by carrying out discrete fast Fourier transform, to find their individual phases and the relative phase difference.

3. Materials and stack specifications

The interaction between the compressible fluid undergoing an acoustic oscillation and solid structures is closely related to two characteristic lengths (Swift, 2002): the viscous penetration depth, defined as

$$\delta_v = \sqrt{\frac{2\mu}{\rho\omega}} \tag{1}$$

and the thermal penetration depth, defined as

$$\delta_\kappa = \sqrt{\frac{2\kappa}{\rho c_p \omega}} \tag{2}$$

Here, μ and κ are the dynamic viscosity and the thermal conductivity of the fluid. ρ is the density and c_p is the thermal capacity of the fluid. ω (= $2\pi f$) is the angular frequency of the acoustic oscillation. Given air at atmospheric pressure and room temperature as the working fluid in the resonator, the viscous penetration depth is 0.26 mm and the thermal penetration depth is 0.31 mm at the operating frequency of 72 Hz. The fluid within this distance from the solid structures experiences the viscous and heat transfer effects. The packing density of the stack material is controlled so that the stack performance can be related to the thermal penetration depth.

Among the selected random materials to be examined are stainless steel wool (Fig. 2a), copper scourers (Fig. 2b) and carbon foam (Fig. 2c). To hold the random materials, a rectangular box of the dimension of a stack was constructed out of 0.5mm thick perforated sheet and used as the casing, as shown in Fig. 2c. In addition, three parallel plate stacks were put to the test, to establish reference cases. Among

them, one was fabricated from Mylar sheets (Fig. 2d) and the other two out of stainless steel plates with different spacing between the plates (Fig. 2e).

3.1. Stainless steel wool

Four stacks were made out of stainless steel wool. The steel wool has very irregular cross sectional area. A sample of 345 pieces of steel wool wire was examined. The details of the examination were already described by Abduljalil et al. (2011). The cross sectional area, A, and the perimeter, Π, were measured as 4329 (± 34%) μm^2 and 311 (± 17%) μm. To make each stack, the steel wool of a given amount was packed in the box as evenly as possible, and in such a way that the orientation of most of the steel wool wires is along the direction of the acoustic oscillation. The hydraulic radius is a parameter used to characterize the packing density of these random materials.

The hydraulic radius, r_h of a stack is normally defined as the ratio of the volume in the stack taken by the gas V_{gas} to the total wetted area of the stack, A_{wet}, as follows.

$$r_h = \frac{V_{gas}}{A_{wet}} \tag{3}$$

The volume of gas in the stack V_{gas} is the difference between the total volume of the stack, V_{tot} and the effective volume occupied by the solid material, V_{solid}, and $V_{solid} = m_{solid}/\rho_{solid}$, where m_{solid} and ρ_{solid} are the mass and the density of the solid material. To obtain the total wetted area of the stack of steel wool, it is assumed that each wire of the steel wool has constant cross-sectional area, A and perimeter, Π. Thus, the wetted area of the stack, A_{wet} can be obtained from

$$A_{wet} = \frac{m_{solid}}{\rho_{solid}} \frac{\Pi}{A} \tag{4}$$

Combining Eqns. (3) and (4), the hydraulic radius of the stack made from steel wool is calculated as follows.

$$r_h = \frac{V_{tot} - \frac{m_{solid}}{\rho_{solid}}}{\frac{m_{solid}}{\rho_{solid}} \frac{\Pi}{A}} \quad (5)$$

The amount of steel wool used to make stacks varies from 104.0 to 269.0 grams, which gives a ratio of the hydraulic radius to the thermal penetration depth between 1.1 and 3.0.

3.2. Copper scourers

In addition, four stacks were made out of copper scourers. Compared with the steel wool, the wire of the copper scourers used is generally of a relatively uniform rectangular cross section and thicker. A sample of 75 pieces of copper scourers wire was examined. The thickness was measured as 61.7 (± 17%) µm and the width as 580.0 (± 15%) µm. Based on propagation of uncertainty, the cross sectional area, A, and the perimeter, *Π*, of copper scourers wires are estimated to be 35770 (± 32%) $(\mu m)^2$ and 1283 (± 16%) µm. The surface area to mass ratio of the copper scourers sample is 4.02 $m^2\ kg^{-1}$, compared to 8.96 $m^2\ kg^{-1}$ for the steel wool.

The copper scourers usually come in a woven pattern and rolled into a doughnut shape (Fig. 2b). To pack it into the stack casing, each of the copper scourers is firstly unrolled into a single layer and then pressed into the casing one by one. The hydraulic radius of a stack made from copper scourers can also be estimated by using Eq. (5). The amount of copper scourers used in the range of 120 and 219 grams produces a ratio of the hydraulic radius to the thermal penetration depth, r_h/δ_κ between 2.8 and 5.8. A smaller value of r_h/δ_κ was not possible to achieve due to the difficulty of packing a greater mass into a given volume.

3.3. Carbon foam

Two other stacks were fabricated from reticulated vitreous carbon (RVC) foam (Duocel®, ERG Aerospace Corp.). RVC foam is tested as a good example of carefully fabricated 'random' material, which has filaments in all directions, in contrast to steel wool and copper scourers. The pre-formed carbon foam will allow a relatively small value of r_h/δ_κ to be achieved. In order to find the hydraulic radius of the RVC foam samples, Eq. (3) has been applied. The specific surface area, that is, the surface area per unit volume, of the RVC foam is estimated from the product specification, as shown in Fig. 3. The relative density, defined as the ratio of the foam density and the bulk density of the material, is typically 3%. Based on this information, for the two carbon foam stacks under test (45 and 60 PPI), the ratio of the hydraulic radius to the thermal penetration depth, r_h/δ_κ, is 1.14 and 0.867, respectively.

3.4. Parallel plate stacks

In addition, three parallel plate stacks were made; one was made of Mylar sheets (Fig. 2d) and two were made of stainless steel sheets (Fig. 2e). Mylar sheets have a thickness of 0.1 mm and the spacing between sheets is 0.7 mm. This material was chosen for its low thermal conductivity, thus low conduction loss, in comparison to stainless steel sheet.

The steel sheets are 0.5 mm and 0.2 mm thick, respectively. The spacers form channels of 1.2 mm and 0.9 mm height, respectively. The fabrication procedures for the parallel plate stacks are similar to those described by Tijani (2002). The three parallel plate stacks were tested and used as reference configurations in comparison with the stacks made from 'random' materials.

The specifications of all stacks are summarized in Table. 1. It is worth pointing out here that the hydraulic radii obtained for the selected 'random' materials only indicate an average packing density

and should only be used as a nominal value for characterization purpose. Also given in the table are the values of the ratio of the hydraulic radius to the thermal penetration depth, r_h/δ_k.

4. Characteristics of thermoacoustic refrigerator

To build the confidence in the operation of the resonator and the acoustic field established, the acoustic characteristics of the resonator alone (without the heat exchangers and stack) were firstly studied by measuring the acoustic pressure amplitude along the resonator. Its distribution was compared with the results from simulation by using DeltaEC. This design tool is capable of solving one dimensional acoustic wave equation, together with the energy equation to map out one dimensional distribution of acoustic velocity, pressure and mean temperature in the whole system (Ward and Swift, 1994). Fundamental parameters such as the amplitude and phase of acoustic pressure and velocity and mean temperature in the main components of a thermoacoustic system can be obtained from the simulation.

The measured pressure amplitude along the resonator is illustrated by the symbols in Fig. 4. At the operating frequency of 72 Hz, the pressure node and the velocity anti-node of the acoustic field in the resonator is at the location of the compliance box. The distributions of the acoustic pressure amplitude and the volumetric velocity amplitude in the resonator obtained from simulation are indicated by the solid line in Fig. 4, with x = 0 defined as the location of the loudspeaker. It can be seen from the pressure and velocity distributions that, the pressure anti-node is about 1.1m from the loudspeaker, where the velocity amplitude also reaches a minimum. The difference in pressure between the simulation and the measurement is less than 5%.

It is also confirmed from the measurement of the acoustic pressure in the resonator that the harmonics in the acoustic resonator are negligible. Thus, it is considered to be appropriate to evaluate the acoustic power delivered by the loudspeaker, W_{ac} using the following equation

$$W_{ac} = \frac{1}{2}|p||U|\cos(\Phi_{pU}) \tag{6}$$

where |p| is the amplitude of the acoustic pressure of the fundamental frequency. |U| is the volumetric velocity amplitude of the generated oscillatory flow on the surface of the loudspeaker, and Φ_{pU} is the phase difference between the pressure and velocity oscillation. The volumetric velocity amplitude can be derived from

$$|U| = \omega A_{spk}|\xi| \tag{7}$$

where ω is the angular frequency. A_{spk} and $|\xi|$ are the cross-sectional area and the displacement amplitude of the diaphragm of the loudspeaker, respectively. Also, it is known that the phase of velocity is 90° leading the phase of displacement. Therefore, Eq. (6) can be rewritten as

$$W_{ac} = \frac{1}{2}|p|\omega A_{spk}|\xi|\cos(\Phi_{p\xi} - 90°) \tag{8}$$

$\Phi_{p\xi}$ is the phase difference between the pressure and displacement oscillation. Thus, the acoustic power delivered to the resonator can be calculated from the acoustic pressure in front of the diaphragm, the displacement of the diaphragm and the phase difference between these two variables, which are directly obtained from the measurements.

The performance of a thermoacoustic refrigerator can be evaluated by the cooling coefficient of performance (COP), defined as

$$COP = \frac{Q}{W_{ac}} \tag{9}$$

Q is the cooling load. W_{ac} is the acoustic power delivered to the system. The coefficient of COP clearly indicates the amount of heat, Q, removed from the cold reservoir by spending useful work W_{ac}. To compare the thermal performance, it is also required to know the temperature of the cold reservoir and the temperature difference that refrigerators have to overcome. As the temperature at the cold end of the

stack was created by the cooling effect, instead of being controlled, the information of the temperature of the cold reservoir is not reflected in the value of COP. In this case, the removed heat, Q can be high when there is a small temperature difference to overcome, which then leads to a large value of COP. In order to make meaning comparison of thermodynamic performance, it is also necessary to consider the Carnot COP, and the ratio of COP to it, as explained below.

The Carnot COP (COPC) is the highest COP that a refrigerator can possibly achieve between two given operating temperatures T_c and T_h, that is, the Carnot's theoretical limit. T_c is the temperature of the cold reservoir, and T_h is that of the hot reservoir. The Carnot COP is defined as

$$\mathrm{COPC} = \frac{T_c}{T_h - T_c} \tag{10}$$

The temperatures measured at the cold and hot ends of a stack are used as T_c and T_h, to exclude the effect of heat transfer efficiency of the heat exchanger. To account for the difference in the performance of a refrigerator operating at different temperatures, and to enable the evaluation of the performance of refrigerator with different stacks, the ratio of COP to Carnot COP, COPR, is introduced in the following analysis, which is defined as

$$\mathrm{COPR} = \frac{\mathrm{COP}}{\mathrm{COPC}} \tag{11}$$

5. Results and discussion

The comparisons between the stacks under investigation are given using standardised graphs including COP vs. cooling load, COPR vs. cooling load, temperature difference vs. cooling load and also maximum COPR vs. r_h/δ_κ. Sections 5.1 – 5.4 deal with stainless steel wool, copper scourers, carbon foam, and parallel plate stacks, respectively. Section 5.5 deals with measurement uncertainty followed by additional remarks in section 5.6.

5.1. Stainless steel wool

The values of COP and COPR of the thermoacoustic refrigerator facilitated with each of the four steel wool stacks are plotted against the cooling load in Fig. 5. As can be seen, the dependence of COP on cooling load is almost linear. This is because the input acoustic power does not change significantly when different cooling loads were applied to each stack tested. It seems that the small change in the temperature at the cold end of the stack and the cold heat exchanger (i.e. cooling load) has little effect on the fluid dynamics in the resonator. However, between stacks, the input acoustic power consumed was slightly different, which can be seen from the different slopes in the linear dependence (Fig. 5a).

When there is no effective cooling load applied on the cold heat exchanger, COP becomes null for all tested steel wool stacks. All lines will converge to the zero point. However there is still acoustic power consumed, which is used to overcome the viscous effect within the steel wool stacks and to remove the heat conducted in the solid along the temperature gradient to the cold end of the stack and any heat leakage from the surroundings. COPR is also null because of a zero COP.

For the same cooling load, the values of COP are in general slightly higher for steel wool stacks having values 2.0 and 3.0 of r_h/δ_k. It is considered that the higher COP value is a result of a lower acoustic power consumed in the stack, which consists of a large number of fine wires interweaving with each other and dissipating acoustic power. However, the values of COP do not decrease monotonically with the decrease of r_h/δ_k, due to the nature of steel wool being random interwoven material; it is very difficult to pack each stack with the wool evenly distributed within the designated volume. In this sense, the calculated hydraulic radius, r_h can only represent an averaged ratio of the gas volume to the

total wetted area of the stack. This is why more acoustic power is not always required for a stack having a smaller r_h/δ_k. For example, the values of COP are very similar for both steel wool stacks having values 1.1 and 1.5 of r_h/δ_k. However, steel wool stack with 1.5 of r_h/δ_k has indicated a lower performance in terms of the COPC, COPR and $(T_h - T_c)$. The performance of the refrigeration will depend, to certain extent, on how evenly the stack is packed. It is more of the case for a densely packed stack, i.e. one that has a smaller r_h/δ_k.

For each of the steel wool stacks tested, the value of COPR firstly increases with the increase of the cooling load and then decreases (Fig. 5b). There is a value of r_h/δ_k associated with a maximum COPR for every steel wool stack. The maximum COPR exists because, while COP increases almost linearly with the cooling load, COPC increases faster. This is due to the fact that the difference in temperatures between two ends of the stack, $(T_h - T_c)$, decreases quickly with the increase of the cooling load (Fig. 5c), and the cold end temperature of the stack, T_c increases as well. At certain point, the temperature difference between two ends of the stack eventually approaches zero (when there is no effective cooling effect for any benefit), and the value of COPC becomes infinite and COPR null. The maximum values of COPR are 0.13% and 0.12% for stacks having r_h/δ_k 2.0 and 1.1, respectively. These values are very small, in comparison with conventional refrigeration technology, such as vapour compression refrigeration, which can be as much as 60%. In summary, results show that there are optimal values of COP, COPC and COPR that can be achieved at a certain ratio of r_h/δ_k. In this case this is 2.0. However, a ratio of 1.1 for r_h/δ_k might be preferred with steel wool stacks, to take advantage of a larger temperature difference on the stack and relatively high COPR.

5.2. Copper scourers

Figure 6 shows the values of COP and COPR of the thermoacoustic refrigerator, when it was equipped with one of the four stacks of copper scourers. The variation of both COP and COPR with the change in cooling load generally resembles what can be observed for the steel wool stacks. The values of r_h/δ_κ for the stacks made of copper scourers are relatively higher than those of steel wool stacks, due to the fact that the copper scourers wires are quite thick and woven in a pattern.

For stacks made of copper scourers, the values of COP, COPR and temperature differences are generally higher when r_h/δ_κ is smaller, except for one stack with r_h/δ_κ at 3.9, which appears to have the lowest performance (see Fig. 6). The general trend of the variation of the COP, COPR, temperature differences and maximum COPR with the change of r_h/δ_κ for the copper scourers stacks seems almost a further extension to that for steel wool stacks (Fig. 5 and 6).

The performance of the steel wool stacks is generally higher than the performance of copper scourers stacks. With the steel wool stacks a maximum temperature difference, (T_h - T_c), of 7.2 ºC was achieved, whereas the copper scourers stacks only reached a maximum temperature difference of 2.8 ºC between the stack ends. This is most probably due to the limits in the hydraulic radius achievable using the simple packing method to construct the copper scourers stacks. A comparison can be made between the copper scourers stack having r_h/δ_k = 2.8 and the steel wool stack having r_h/δ_k = 3.0. The maximum temperature difference between stack ends for the former stack, (T_h-T_c) is 2.8 ºC while for the latter stack it was 4.9 ºC.

5.3. Stacks of carbon foam

From the viewpoint of the heat transfer between the working fluid and the stack, it is normally beneficial to have a large surface area for a given stack volume (Swift, 2002). This is equivalent to a

smaller hydraulic radius for the given stack volume. It is also preferred to have stacks made of a material that has low thermal conductivity, and high product of heat capacity and density. With these consideration, the commercially available RVC foam was chosen to represent 'carefully designed' isotropic porous materials. RVC foams of 60 PPI and 45 PPI were selected. The former one has the smallest r_h/δ_κ of 0.867 in this series of test, while the latter sample has r_h/δ_κ of 1.14, which is close to the smallest r_h/δ_κ (of 1.1) achieved by the steel wool stacks.

From Figure 7 it can be seen that, the RVC foam stack of 60 PPI has a better thermal performance than the other stack, due to a smaller r_h/δ_κ. When compared to the results of copper scourers stacks, both RVC foam stacks can take a slightly higher cooling load than all stacks of copper scourers, with equivalent or marginally higher temperature differences. RVC foam stacks also consume slightly more acoustic power, hence a bit lowered COP at the same cooling load. The COPR for RVC foam stacks is a bit higher than in the results for stacks of copper scourers. This slightly better thermal performance of the RVC foam stacks probably mainly attributable to the smaller ratios of r_h/δ_κ.

When comparing the RVC foam stack of 45 PPI, which has r_h/δ_κ of 1.14, with the steel wool stack of r_h/δ_κ = 1.1, it can be seen that the thermal performance of the steel wool stack is remarkably higher. Between the two types of stacks, the difference lies in the material, as well as the orientation of the filaments due to the packing method, and the topology of the voids in which the gas moves. It is not clear which factor plays a more important role.

5.4. Parallel plate stacks

As shown in Fig. 8, the values of COP, COPR and (T_h - T_c) for both steel parallel plate stacks show a very similar trend, while the values for the Mylar parallel plate stack with r_h/δ_k at 1.3 are significantly

higher. The stainless steel sheet used to fabricate the stack has relatively high thermal conductivity. It can be speculated that the remarkably higher performance of the Mylar stack is a result of relatively low thermal conductivity which makes the unwanted heat conduction along the wave propagation direction smaller.

For the Mylar parallel plate stack, the temperature difference over the stack ends, and the values of COPR are the highest among all the stacks tested, whereas the stainless steel plate stacks are only comparable or slight worse than the steel wool stacks.

5.5. Measurement uncertainty

Among the quantities used for the calculations of COP and COPR, the temperatures at both ends of the stacks are directly measured with uncertainty of 0.2 °C. The acoustic power is calculated from the acoustic pressure amplitude, the displacement amplitude and the phase difference between these two. The relative uncertainty of the acoustic power is not more than 4.75%. The cooling load is deduced from the measured voltage and current, with a relative uncertainty less than 0.45%. Therefore, the relative uncertainty of the calculated COP is under 4.78%.

The uncertainty of COPC can be calculated using the following equation

$$\sigma_{\mathrm{COPC}}^2 = \left|\frac{\partial \mathrm{COPC}}{\partial \mathrm{T_h}}\right|^2 \sigma_{\mathrm{T_h}}^2 + \left|\frac{\partial \mathrm{COPC}}{\partial \mathrm{T_c}}\right|^2 \sigma_{\mathrm{T_c}}^2 \tag{15}$$

From Eq. (13), the relative uncertainty of COPC can be derived as

$$\left(\frac{\sigma_{\mathrm{COPC}}}{\mathrm{COPC}}\right)^2 = \left(\frac{\mathrm{T_h}}{\mathrm{T_h}-\mathrm{T_c}}\right)^2 \left[\left(\frac{\sigma_{\mathrm{T_h}}}{\mathrm{T_h}}\right)^2 + \left(\frac{\sigma_{\mathrm{T_c}}}{\mathrm{T_c}}\right)^2\right] \tag{16}$$

The uncertainty of COPC is related to the difference between T_c and T_h. The smaller the temperature difference (T_h - T_c), the larger the uncertainty would become. When the cooling power increases, the temperature difference (T_h - T_c) would even approach 0 °C, and the relative uncertainty could be well over 250%. However, in the determination of maximum COPR, the maximum value of COPR usually appears when the cooling load is not more than 3.0 W. In this case, the relative uncertainty of COPC is less than 16.7%. Accordingly, the relative uncertainty of maximum COPR is not more than 17.4%.

5.6. Final remarks

In order to achieve an optimal performance for a thermoacoustic refrigerator, it is usually preferred to make the stacks of materials that have low thermal conductivity in the wave propagation direction, and high product of heat capacity and density, or high ρc/k values. The stacks are also required to have high specific surface area with regular channels to minimise the acoustic power consumption. Due to the nature of the investigation of stacks made from random materials, that are readily available, low cost and/or waste materials, it is not possible to control all the stack parameters for a fully comprehensive comparison both within the same type of material and between different types. The use of ratio, r_h/δ_κ is a widely accepted way to quantify the geometry of the stack, with considerations given to both the specific surface area and the flow channels. However, clearly, it has its own limitations, as indicated by the experimental results.

From the experimental study of a thermoacoustic refrigerator equipped with carefully fabricated parallel plate stacks and pressurised helium as the working gas, Tijani et al. (2002) concluded that the r_h/δ_κ of stacks needs to be controlled at specific values in order to reach optimal output from the

refrigerator. A stack that has r_h/δ_κ of 1.25 (equivalent to a plate spacing of 2.5 times δ_κ) was found to have the maximum cooling power, and one that has r_h/δ_κ of 2 was able to achieve a lowest temperature, while r_h/δ_κ of 1.5 seems to give the best overall performance (Tijani et al., 2002). The results presented in this paper for stacks made of random materials (i.e. stainless steel wool and copper scourers) are to some extent similar in trend, however, the values are usually orders of magnitude lower. Compared to the stacks of random material, the parallel plate stacks used in this study, confirmed that better performance can be achieved in terms of higher values of COP and COPR.

However, the stacks of random material have certain advantages with regard to the cost associated with the material and the manufacturing process. Generally a stack of steel wool weighing 500 grams can be purchased from almost any metal works manufacturer for approximately £5 (≈ $8) to £10 (≈ $16), as it is considered a waste material (but usable in areas such as cleaning), whereas a parallel plate stack of the same dimensions is likely to cost ten times the price of the steel wool stack. It is also worth emphasising that the current investigation is not intended to suggest that the use of a random material stack is required to achieve the optimum efficiency, but to present the benefits of implementing stacks of waste materials for use in thermoacoustic coolers, when a cost-effective device becomes an option with acceptable compromise in efficiency.

6. Conclusion

In this paper, the experimental method to evaluate the thermal performance of stacks in a standing wave thermoacoustic refrigerator is described. Random stack materials such as stainless steel wool, copper scourers and preformed reticulated vitreous carbon foam were tested. Furthermore, stacks made from Mylar sheets and stainless steel sheets were used as reference test cases. The experimental results reveal that among the tested random stack materials, the steel wool stacks with r_h/δ_k of 2.0 and 1.1

achieved the maximum cooling power, the lowest temperature and the highest COPR. Other random material stacks underperform the steel wool stacks, which is partially due to higher values of r_h/δ_k. This is particularly the case for copper scourers stacks, caused by the difficulty in packing with the current packing method.

For the parallel plate stacks, Mylar sheets stack clearly showed a better performance in comparison to both parallel plate stacks and random material stacks. It achieved a maximum COP, COPR and a temperature difference of 0.217, 0.15% and 7.7 °C, respectively. Further analysis of the hydrodynamic and thermoacoustic characteristics of the tested materials would be beneficial to improve the thermal performance of such a thermoacoustic refrigerator equipped with a stack made of random material, when a low cost device with slightly lower performance found its application.

Acknowledgement

This work has been supported by the Engineering and Physical Sciences Research Council (EPSRC) through grant EP/E044379 and Royal Society Industry Fellowship for Professor Artur. J. Jaworski (2012-2015). The authors wish to acknowledge the assistance of Mr Harry Holden and Dr Patcharin Saechan in some of the measurements. Samir Gh. Yahya acknowledges the support from the University of Diyala and Higher Committee for Education Development (HCED) in Iraq.

References

Abduljalil, A. S., Yu, Z., and Jaworski, A. J., 2011, "Selection and experimental evaluation of low-cost porous materials for regenerators applications in thermoacoustic engines", Materials and Design, 32, pp. 217-228.

Backhaus, S., and Swift, G. W., 2001, "Fabrication and use of parallel plate regenerators in thermoacoustic engines", Proceedings of 36th Intersociety Energy Conversion Engineering Conference, Vol. 1 of 2, Savannah, GA, United States, 29 July – 2 Aug, pp. 453-458.

Bailliet, H., Gusev, V., Raspet, R., and Hiller, R. A., 2001, "Acoustic streaming in closed thermoacoustic devices", The Journal of Acoustical Society of America, 110(4), pp. 1808-1821.

Biwa, T., Tashiro, Y., and Mizutani, U., 2004, "Experimental demonstration of thermoacoustic energy conversion in a resonator", Physics Review E, 69(6), 066304, pp. 1-6.

Chang, E. J., and Maxey, M. R., 1994, "Unsteady flow about a sphere at low to moderate Reynolds number. Part 1. Oscillatory motion", Journal of Fluid Mechanics, 277, pp. 347-379.

Hofler, T. J., 1986, "Thermoacoustic refrigerator design and performance", PhD Thesis, University of California, San Diego.

Jaworski A.J. and Mao X., 2013, "Development of thermoacoustic devices for power generation and refrigeration", Journal of Power and Energy, Proceedings of the IMechE – Part A, 227(7), pp. 762-782.

Jebali F., Lubiez J. V., Francois M.-X., 2004, "Response of a thermoacoustic refrigerator to the variation of the driving frequency and loading", International Journal of Refrigeration, 27, pp. 165-175.

Materials and Aerospace Corporation (ERG). (2016) Retrieved 12 July, 2016, from http://www.ergaerospace.com/index.html

Paek I., Braun J. E., Mongeau L., 2007, "Evaluation of standing-wave thermoacoustic cycles for cooling applications", International Journal of Refrigeration, 30, pp. 1059-1071.

Saechan, P., Yu, Z., and Jaworski, A. J., 2011 Optimal design of coaxial travelling wave thermoacoustic cooler, Proc. 23rd IIR International Congress of Refrigeration, Paper ID 590, 21-26 August 2011, Prague, Czech Republic

Swift, G. W., Thermoacoustics: A unifying perspective for some engines and refrigerators, 2002, Acoustical Society of America, Melville, NY.

Tijani M.E.H., Zeegers J.C.H., de Waele A.T.A.M., 2002, "The optimal stack spacing for thermoacoustic refrigeration", Journal of the Acoustical Society of America, 112(1), pp. 128-133.

Wang, C.-Y., 1968, "On high-frequency oscillatory viscous flows", Journal of Fluid Mechanics, 32(1), pp. 55-68.

Ward, W. C. and Swift, G. W., 1994, "Design environment for low-amplitude thermoacoustic engines", Journal of Acoustical Society of America, 95, pp. 3671.

Wetzel, M., Herman, C., 1997, "Design optimization of thermoacoustic refrigerators", International Journal of Refrigeration, 20(1), pp. 3-21.

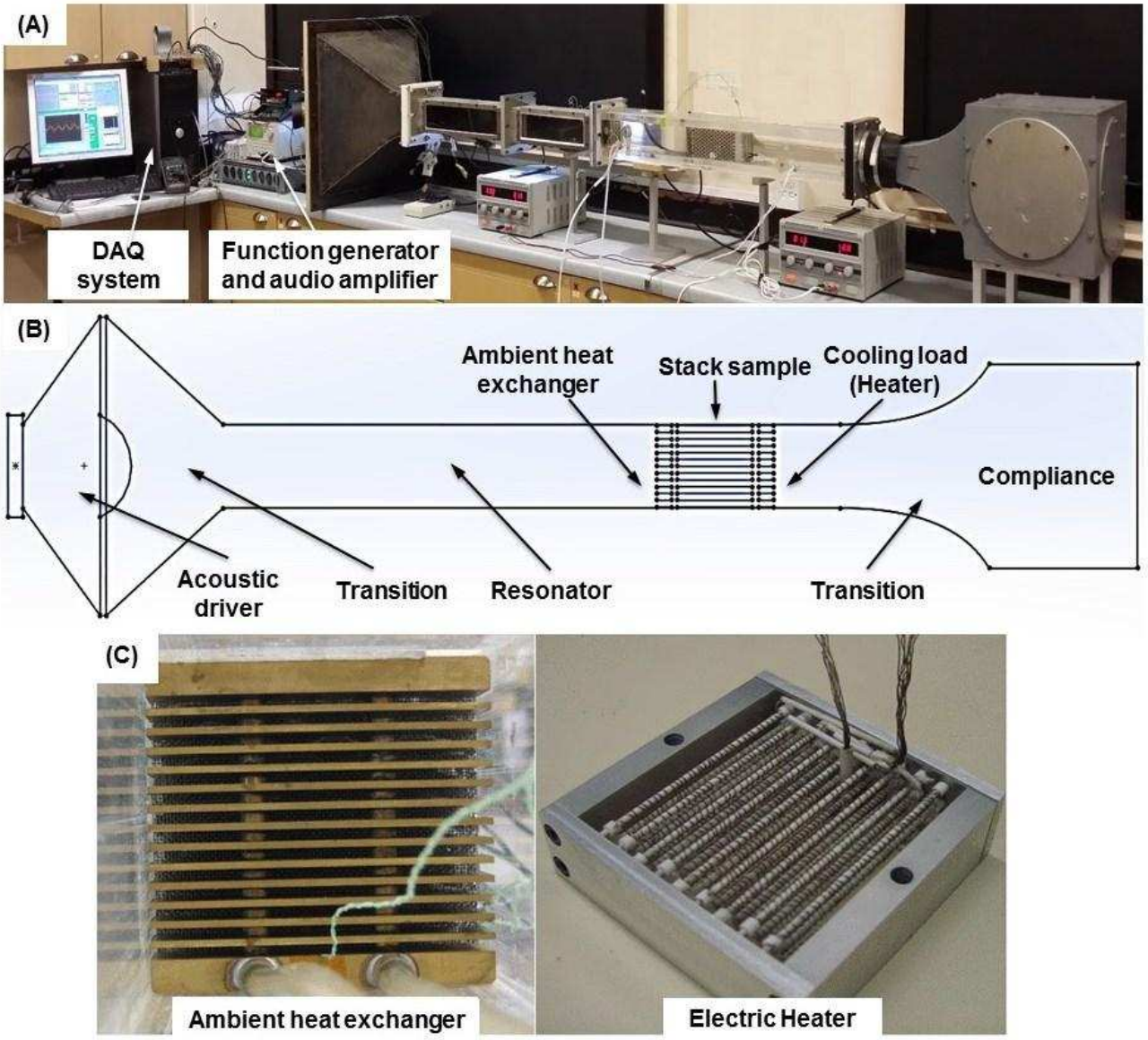

Figure 1 Photograph (A) and schematic (B) of experimental apparatus. Ambient heat exchanger and cold heat exchanger (i.e. electric heater used as cooling load) are illustrated in (C)

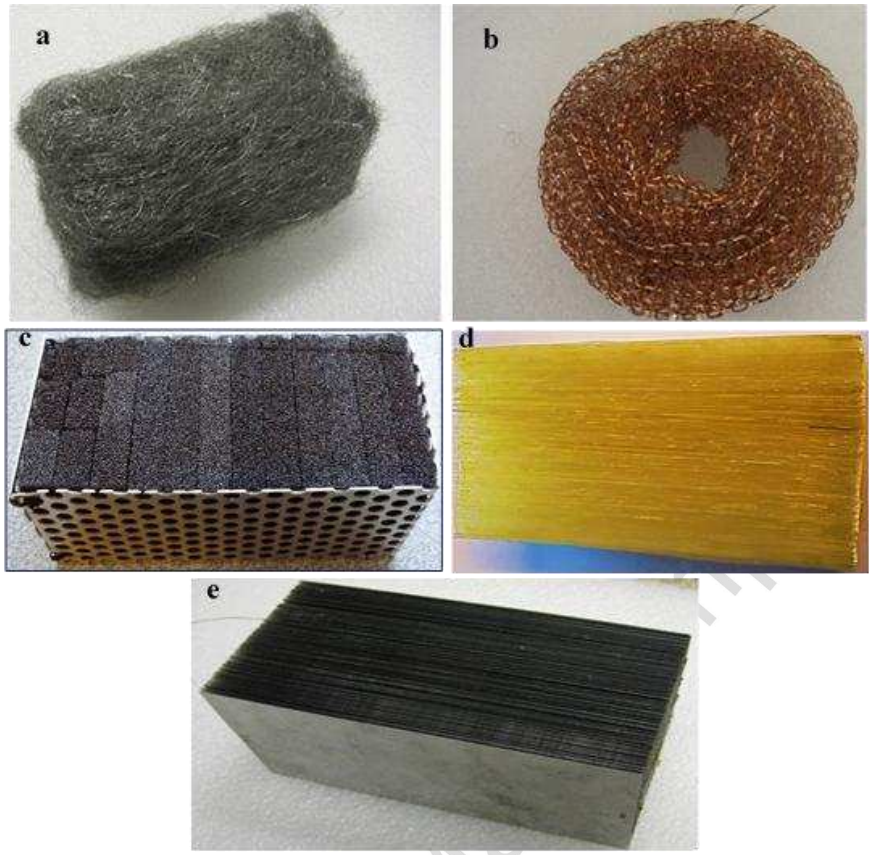

Figure 2 Stack samples: stainless steel wool (a), copper scourers (b), carbon foam (c), Mylar stack (d) and stainless steel stack (e).

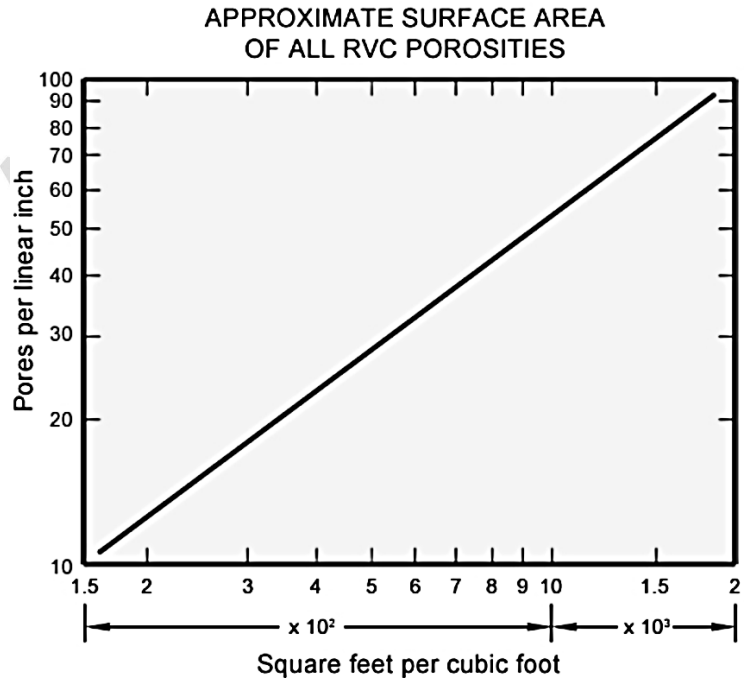

Figure 3 Specific surface area of reticulated vitreous carbon (RVC) foam [ERG Aerospace Corp.**]**

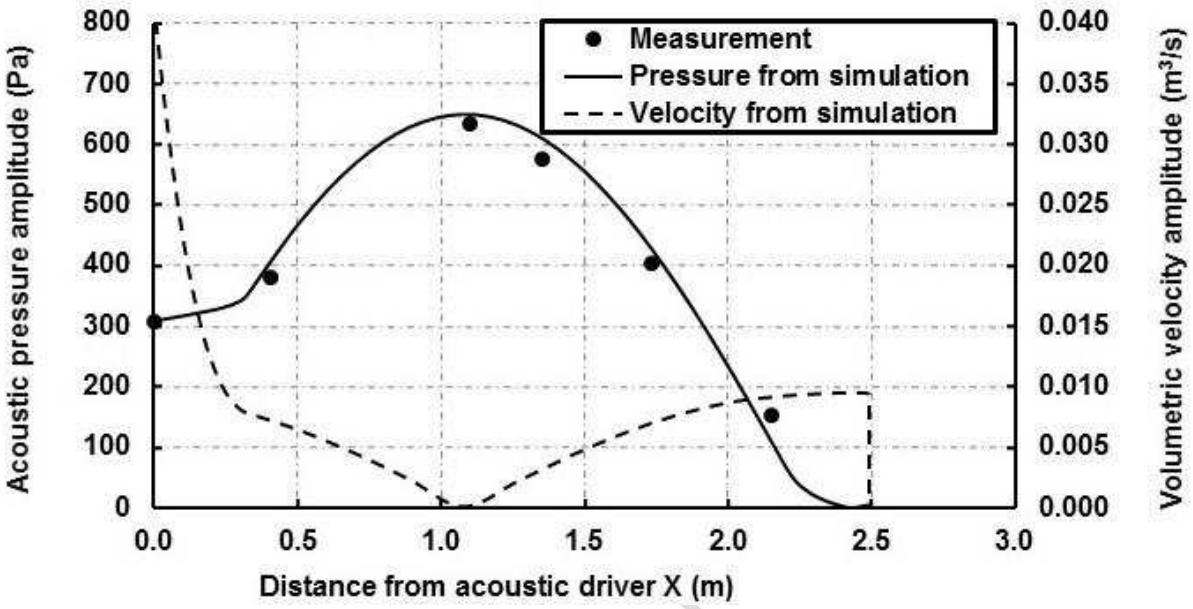

Figure 4 Amplitude of acoustic pressure and velocity in the resonator

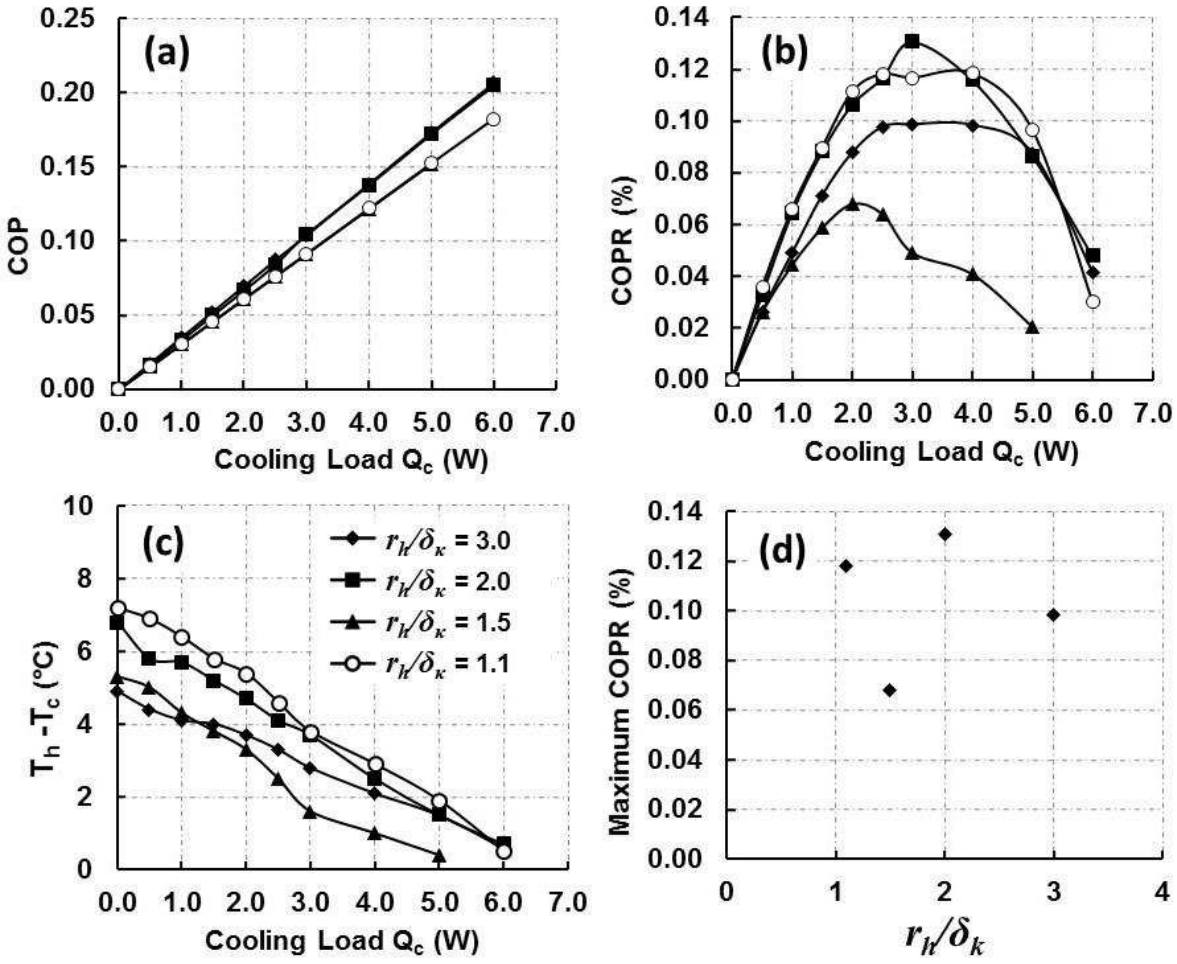

Figure 5 Performance of thermoacoustic refrigerators with steel wool stacks, (a) COP, (b) COPR (%), (c) difference of temperatures at stack ends, (d) maximum COPR (%).

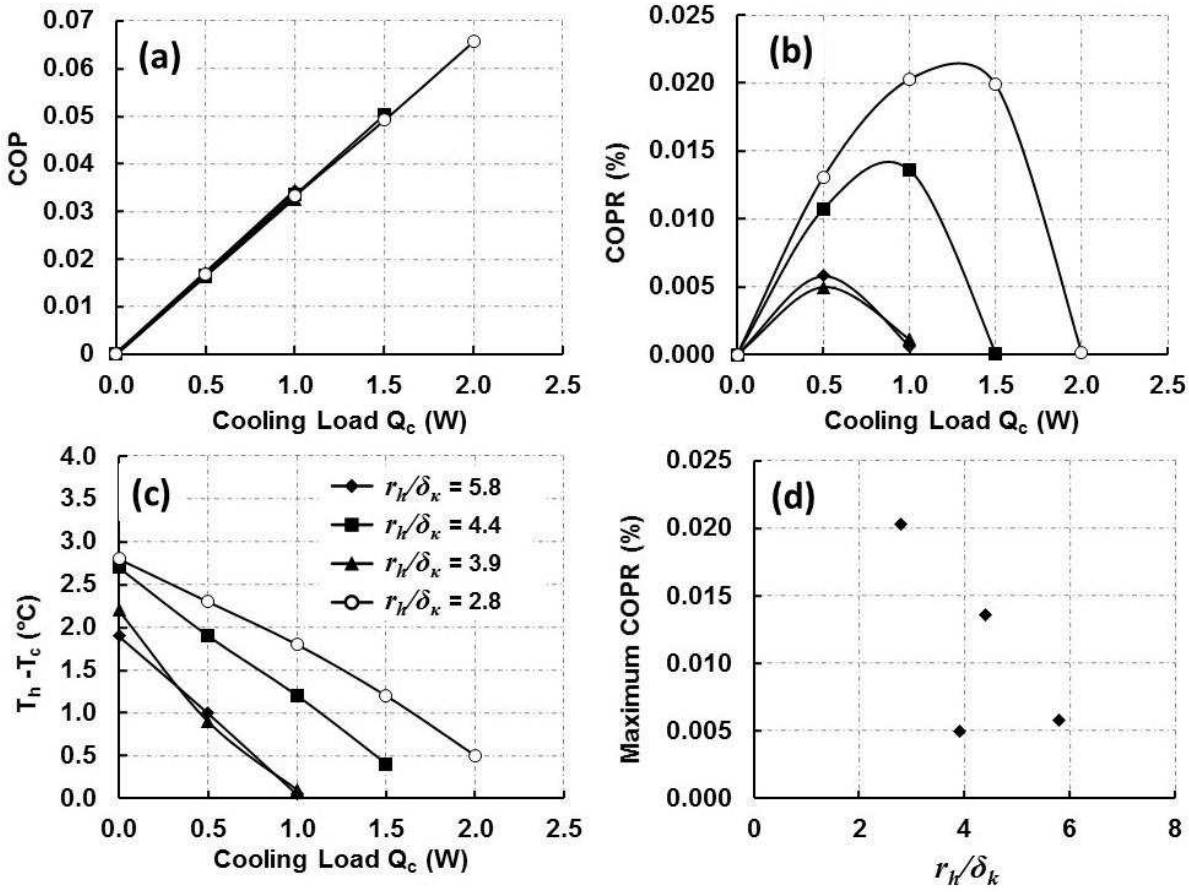

Figure 6 Performance of thermoacoustic refrigerators with copper scourers stacks, (a) COP, (b) COPR (%), (c) difference of temperatures at stack ends, (d) maximum COPR (%).

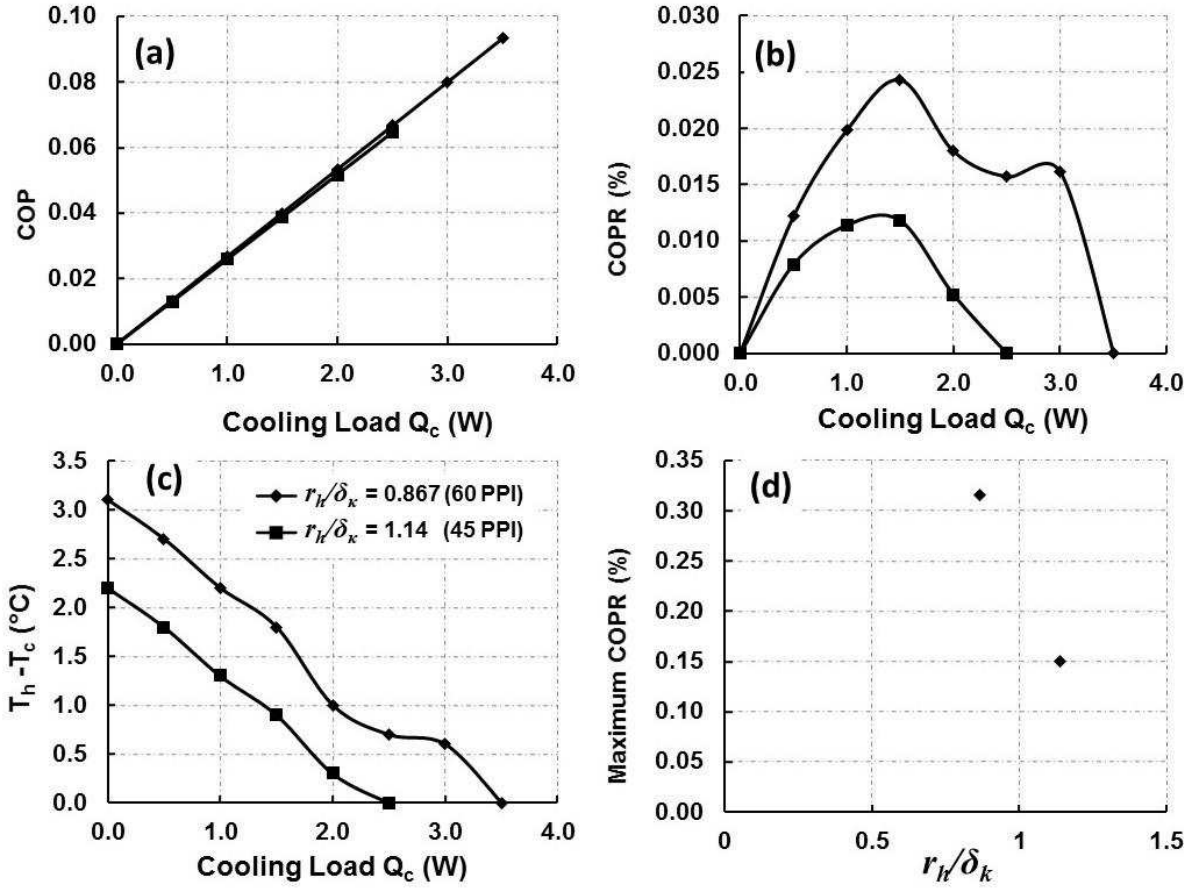

Figure 7 Performance of thermoacoustic refrigerators with reticulated vitreous carbon foam stacks, (a) COP, (b) COPR (%), (c) difference of temperatures at stack ends, (d) maximum COPR (%).

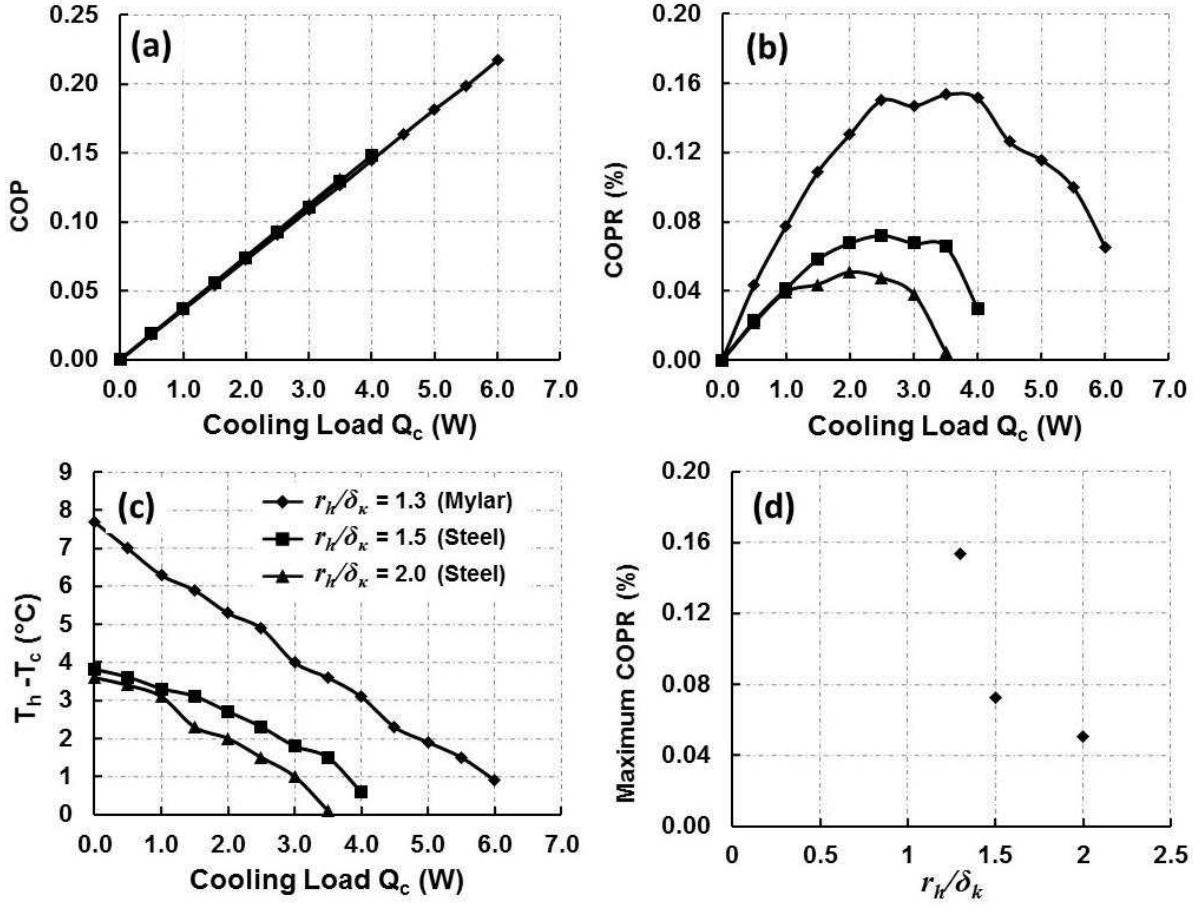

Figure 8 Performance of thermoacoustic refrigerators with parallel plate stack, (a) COP, (b) COPR (%), (c) difference of temperatures at stack ends, (d) maximum COPR (%).

Table 1. Specifications of stacks

Material of stack	Mass (grams)	r_h	r_h/δ_k
Steel wool 1	104	0.921	3.0
Steel wool 2	154	0.614	2.0
Steel wool 3	210	0.449	1.5
Steel wool 4	269	0.348	1.1
Copper scourers 1	120	1.779	5.8
Copper scourers 2	156	1.362	4.4
Copper scourers 3	177	1.197	3.9
Copper scourers 4	219	0.867	2.8
PPI			
RVC Foam 1	45	0.352	1.14
RVC Foam 2	60	0.269	0.867
Plate thickness (mm)			
Steel plate 1	0.5	0.60	2.0
Steel plate 2	0.2	0.45	1.5
Mylar sheets	0.1	0.4	1.3